

Simple and practical sialoglycan encoding system reveals vast diversity in nature and identifies a universal sialoglycan-recognizing probe derived from AB₅ toxin B subunits

Aniruddha Sasmal^{1,2}, Naazneen Khan^{1,2}, Zahra Khedri^{1,2}, Benjamin P. Kellman³, Saurabh Srivastava^{1,2}, Andrea Verhagen^{1,2}, Hai Yu⁵, Anders Bech Bruntse³, Sandra Diaz^{1,2}, Nissi Varki^{1,2}, Travis Beddoe⁶, Adrienne W. Paton⁷, James C. Paton⁷, Xi Chen⁵, Nathan E. Lewis^{1,3} and Ajit Varki^{1,2,4}

¹Glycobiology Research and Training Center, ²Department of Cellular & Molecular Medicine, ³Department of Pediatrics, and ⁴Department of Medicine, University of California, San Diego, La Jolla, CA-92093, ⁵Department of Chemistry, University of California, Davis, CA, 95616, USA, ⁶Department of Animal, Plant and Soil Science and Centre for AgriBioscience, La Trobe University, Bundoora, Victoria 3086, Australia, and ⁷Research Centre for Infectious Diseases, Department of Molecular and Biomedical Science, University of Adelaide, Adelaide, SA 5005, Australia.

Encoded sialoglycan microarray study of AB₅ toxin B subunits

*Address correspondence to:

Ajit Varki
Email: a1varki@ucsd.edu
UCSD School of Medicine
La Jolla, CA 92093-0687

Keywords

Glycan microarray, glycan coding, bacterial toxin, toxin B subunit, *Yersinia enterocolitica*.

Supplementary Data includes Figures. S1-S3, Table SI-SII, and Microarray data.

Abstract

Vertebrate sialic acids (Sias) display much diversity in modifications, linkages and underlying glycans. Slide microarrays allow high-throughput explorations of sialoglycan-protein interactions. A microarray presenting ~150 structurally-defined sialyltrisaccharides with various Sias linkages and modifications still poses challenges in planning, data sorting, visualization and analysis. To address these issues, we devised a simple 9-digit code for sialyltrisaccharides with terminal Sias and underlying two monosaccharides assigned from the non-reducing end, with three digits assigning a monosaccharide, its modifications, and linkage. Calculations based on the encoding system reveal

>113,000 likely linear sialyltrisaccharides in nature. Notably a biantennary *N*-glycan with two terminal sialyltrisaccharides could thus have $>10^{10}$ potential combinations and a triantennary *N*-glycan with three terminal sequences, $>10^{15}$ potential combinations. While all possibilities likely do not exist in nature, sialoglycans encode enormous diversity. While glycomic approaches are used to probe such diverse sialomes, naturally-occurring bacterial AB₅ toxin B subunits are simpler tools to track the dynamic sialome in biological systems. Sialoglycan microarray was utilized to compare sialoglycan-recognizing bacterial toxin B subunits. Unlike the poor correlation between B subunits and species phylogeny, there is stronger correlation with Sia-epitope preferences. Further supporting this pattern, we report a B subunit (YenB) from *Yersinia enterocolitica* (broad host range) recognizing almost all sialoglycans in the microarray, including 4-O-acetylated-Sias not recognized by a *Y. pestis* orthologue (YpeB). Differential Sia-binding patterns were also observed with phylogenetically-related B subunits from *Escherichia coli* (SubB), *Salmonella* Typhi (PltB), *S. Typhimurium* (ArtB), extra-intestinal *E. coli* (EcPltB), *Vibrio cholera* (CtxB), and cholera family homologue of *E. coli* (EcxB).

Introduction

Glycans play critical roles in numerous structural and modulatory functions in cells. Cell surface glycans are particularly important as they are involved in various biological processes, like cell signaling, host-pathogen interaction, and immune interactions (Lewis et al., 2022; Dhar et al., 2021). Sialic acids (Sias) are nine-carbon monosaccharides that are the most prominent terminal monosaccharides found in mammalian cell surface glycomes. The sialome is defined as the “total complement of sialic acid types and linkages and their mode of presentation on a particular organelle, cell, tissue, organ or organism—as found at a particular time and under specific conditions” (Varki and Angata, 2006). The huge diversity in sialomes arises from the monosaccharide identity, functional modification, and various linkages of Sias. Besides the two most common mammalian Sias, *N*-acetylneuraminic acid (Neu5Ac) and *N*-glycoylneuraminic acid (Neu5Gc), the Sia family includes

ketodeoxynononic acid (Kdn), and neuraminic acid (Neu), which are rarely found in mammalian glycomes.

Glycans are one of the major classes of macromolecules in nature. Due to the structural complexity of glycans compared to the simpler linear sequences of nucleotides and peptides, the development and availability of glycan informatics resources, such as user-friendly nomenclature, structure motif finder, and database are still limited, hindering the advancement of glycan research (Pérez and Mulloy, 2005; Von der Lieth et al., 2004). Unlike nucleic acids and proteins, glycan sequences are also comprised of a large number of possible monosaccharide residues, variable linkages, and branching possibilities (Laine, 1994; von der Lieth, 2004). The possibility of multiple functional modification and linkages on seven out of the nine carbons in Sias made it particularly challenging to establish a functional yet convenient representation of sialosides. The diversity of sialosides increases further when the underlying glycan structures are taken into account.

To partly address this issue, an abbreviated text-based nomenclature describing the glycan structure was established by the IUPAC-IUBMB (International Union for Pure and Applied Chemistry and International Union for Biochemistry and Molecular Biology) (McNaught, 1997). However, this three-letter coding system is ambiguous and not easily transferable to a machine-readable format. Later LINUCS (Linear Notation for Unique description of Carbohydrate Sequences) was developed to address the IUPAC limitations (Bohne-Lang et al., 2001), but it has not had universal acceptance and applications. Several efforts have since been made to develop a comprehensive representation of complex glycan structures (Banin et al., 2002; Shinmachi et al., 2017; Sahoo et al., 2005; Kikuchi et al., 2005) and their associated reaction rules (Kellman et al., 2020), and established an algorithm for the mining of high-complexity glycan motifs involved in biological processes (Klamer et al., 2017). Attempts have been made to implement useful identifiers for explicitly describing the glycan structures in databases like Complex Carbohydrate Structure Database, CarbBank, Consortium for Functional Glycomics (CFG), CarbArrayART (Kellman et al., 2020; Doubet et al., 1989; Doubet and Albersheim, 1992; Hashimoto et al., 2005; Raman et al., 2006; Toukach et al., 2007; Raman et al., 2006; Akune et al., 2022).

Recently, assignment of unique glycan structure identifiers in the GlyTouCan repository (Tiemeyer et al., 2017) has been increasingly accepted by the glycomics community. A graphical representation of glycan structures by the 'Symbol Nomenclature for Glycans' (SNFG) system has also been standardized (Varki et al., 2015).

Automated and high-throughput analytical techniques, such as glycan microarray produces a large amount of glycan binding data (Cao et al., 2020; Padler-Karavani et al., 2012). Considerable efforts have been made to establish proper nomenclature and motif finders for in-depth study of structure and function relationships of glycans (Cholleti et al., 2012; Tang et al., 2015; Coff et al., 2020; Venkataraman et al., 2015). Many recent studies have focused on glycan motif discovery to bring generalizable meaning to lectin array analysis (Klamer et al., 2019; Klamer et al., 2017; Tang et al., 2015), glycan database analysis (Kellman and Lewis, 2021; Hosoda et al., 2018; Klein and Zaia, 2019) and glycoprofile analysis (Benedetti et al., 2017). Functional meaning or biosynthetic feasibility discovered in the existence or enrichment of one motif can be used to create generalizable expectations regarding the functional importance or biosynthetic feasibility of a novel glycan (Bojar et al., 2021). Historically, our groups have been focusing on identifying novel biological roles of terminal Sias and consequently over the years we developed a sialoglycan-focused microarray platform to explore novel biomolecular interactions with the sialosides (Deng et al., 2013; Bensing et al., 2016; Lu et al., 2019). Our extensive sialoglycan inventory includes mostly sialyltrisaccharides with various modification and linkages of Sia. The ever-increasing sialoglycan microarray library demands an efficient structure representation system to streamline the printing, sorting, analysis, and motif-finding processes. The available tools for the systematic analysis of glycan microarray data do not address the variability of the terminal sialic acids on the mammalian glycans (Mehta et al., 2020). A coding-based systematic representation of complex *N*-linked glycans has been reported, however the functional modifications on the terminal Sias were not addressed in detail (Yusufi et al., 2009). Here we demonstrate a simple yet versatile encoding technique for the representation of mainly sialyltrisaccharide structures that will help in suitable structural representation of glycans in a machine-readable digital format and hope this will

benefit the glycoscience community as a whole. The newly developed coding system can also be utilized to calculate the number of possible naturally occurring sialyltrisaccharide structures in mammalian sialome. Although the complexity and the diversity of the sialome make the calculation of the total number of sialoside structures impossible, we believe that our coding approach will help to address the long-standing question regarding the number of possible glycan structures.

This huge number of sialosides in nature along with their immense role in post-translational modifications and protein-binding make them important targets that need to be probed for the understanding of structure and function (Srivastava et al., 2022). Plant-based lectins are traditionally used to probe the sialosides, however they are often limited in recognizing diverse and complex sialic acid linkages and modification. In this study we took advantage of naturally evolved bacterial toxin B subunits to develop a universal probe for the terminal sialic acids irrespective of their linkages and modifications. We already addressed the characterization of an AB₅ toxin B subunit from *Y. pestis* (YpeB) (Khan et al., 2022). The extensive sialoglycan microarray study revealed that YpeB binds to various modified Neu5Ac and Neu5Gc-terminated glycans, except when the terminal Sia was modified with an O-acetyl group at the C-4 position (Khan et al., 2022). Consequently, the idea of using YpeB as a universal Sia-binding probe had to be dismissed. These shortcomings led us to screen the glycan-binding B subunits of AB₅ toxins from phylogenetically-related bacteria in search of a broader Sia binding probe. The *Yersinia* genus encompasses a heterogeneous collection of Gram-negative facultative non-sporulating anaerobic bacteria that are divided into different serological groups based on the antibody reactions to different lipopolysaccharides (O'Loughlin et al., 1990). Only three species of *Yersinia*, *Y. enterocolitica*, *Y. pestis*, and *Y. pseudotuberculosis*, have been known to infect humans. Enteropathogenic *Y. enterocolitica* is a food-borne pathogen, which is the most prevalent in humans, causing a broad range of gastrointestinal syndromes and may cause septicemia and meningitis (Toma and Lafleur, 1974; Black et al., 1978; Kay et al., 1983). Like *Y. pestis*, *Y. enterocolitica* also has a very broad range of host compatibility. Besides humans, the bacteria have also been isolated from rodents, domestic animals (e.g., cattle, pigs, dogs, sheep), and other animals like horse

and deer (Wang et al., 2010). A systematic screening of toxin B subunit of *Y. enterocolitica* (YenB) along with the other phylogeny-based bacterial toxin B subunits on the sialoglycan microarray was pursued to discover a universal probe that recognizes almost all common types of sialoglycans present in the dynamic mammalian sialome.

Results and Discussion

A coding system for individual sialoglycans on the microarray. The importance and coverage of high-throughput glycan microarray technology depend on the number and diversity of glycans present in the specific library. Over the years we developed an extensive library of sialosides for microarray platform. A series of natural and non-natural sialoglycans (see Supplementary data for full list) were synthesized using chemoenzymatic methods (Chen and Varki, 2010). We restricted the sialoside structure primarily in the form of defined trisaccharides, as addressing all the diverse structures of sialosides in nature is beyond anyone's scope. Except for a few non-sialosides, the terminal monosaccharides used are Neu5Ac, Neu5Gc, and Kdn along with their natural modifications. The terminal Sias at the non-reducing end are linked with the underlying glycan structures in α 2-3, α 2-6, and α 2-8 fashion. Terminal Sias are linked to the underlying glycan structures that are usually known to occur in nature (precisely in mammals), for example, Type I (Gal β 1-3GlcNAc β), Type II (Gal β 1-4GlcNAc β), Type III or T-antigen (Gal β 1-3GalNAc α), Type IV (Gal β 1-3GalNAc β), Type VI (Gal β 1-4Glc β), Lewis antigens, Tn-antigen, sulfated GlcNAc, and ganglioside-type structures (Ye et al., 2016). Initially, the individual sialoglycans were assigned with a number (Glycan ID) in the order they were synthesized and stored. The assigned glycan IDs listed in the table (Supp. data Table SI) are semi-random and do not help in streamlining the sorting and analysis of the microarray data. To address these issues, we developed a simple 9-digit machine-readable coding system to easily order the glycans in various logical ways during spreadsheet analyses and to identify glycan-binding motifs (Table I). Due to its terminal position, most of the biological interest lies on the identity of the Sia. Logically, the coding of the glycans starts from the non-reducing terminal Sias followed by their

modifications and linkages. Subsequently, the underlying two monosaccharides (or more) were assigned from the non-reducing end, each with a digit indicating the monosaccharide type, its modifications, and linkage.

The first digit in the 9-digit code represents the terminal Sia identity. Being the most prevalent Sia in mammalian glycomes, Neu5Ac was assigned number 1 followed by its two most important O-acetyl modifications at C-4 (number 2) and C-9 (number 3) positions. It is noteworthy that Neu5Ac with only C7-O-acetyl modification is not stable (Ji et al., 2021) and hence it was not considered as a primary Sia form. Like Neu5Ac, Neu5Gc and its O-acetyl-modified versions were then assigned the number 4 to 6. The less abundant Kdn and its O-acetyl modifications were assigned afterwards to occupy the numbers 7 to 9. To accommodate the non-sialosides in our library, we decided to assign number 0 for the 'no sialic acid' at the non-reducing end of the glycan. We extended the assignment system to accommodate less abundant Sia forms (not present in our library yet). An alphabet (small letter) was assigned to each of the neuraminic acid (Neu), legionaminic acid (5,7-di-*N*-acetyl legionaminic acid, Leg5,7Ac₂), and other nonulosonic acids mostly present in prokaryotes. It is noteworthy that while the existence of 'naked' Leg is theoretically possible, all the naturally occurring legionaminic acids reported thus far are *N*-acylated at C-5 and C-7 positions. These sialoglycans were assigned with letters starting from *a* and filling downwards as the library expands. The second digit in the coding system was to identify the modification on the Sia. We assigned numbers 1 through 9 for each type of naturally occurring O-acetyl, lactone, O-lactyl, 5-O-methyl, and 8-O-methyl modifications on the Sia. To the best of our ability, we tried to rationalize the assignment of the number by matching the carbon position of the specific Sia modification. Number 9 was assigned to the (7/8),9-di-O-acetyl modification where the position for one of the O-acetyl groups is not confirmed due to the O-acetyl migration among C-7, C-8, and C-9 positions (Ji et al., 2021). The 1,5-lactam (Otsubo et al., 2001; Yamaguchi et al., 2003), a modification derived from neuraminic acid (Neu) was assigned with alphabet *a*. Next in the column, the third digit represented the various types of natural linkages connecting the C-2 position of Sia to the next underlying monosaccharide unit in alpha stereochemical fashion. To date, no beta linkage

was reported to occur at the C-2 position of the Sia (except in the CMP-monosaccharide state). Rationally, the α 2-3 connection was assigned to number 3, α 2-6 connection to number 6 and so on. To make the numbering system more self-explanatory, we did not assign number 1 and 2 to any of the linkages, the obvious reason being the absence of α 2-1 and α 2-2 Sia connections. In total, the first three digits in the coding system were sufficient to properly express most Sias at the non-reducing end. Similarly, the next three digits enumerated the identity, modification/branching, and the linkage of the next underlying monosaccharide. In a poly/oligosialic acid, the Sia is linked to another Sia in α 2-8-fashion and for that reason we included Sia in the list of second sugar unit (fourth digit). To keep the numbering system in sync, the Neu5Ac, Neu5Gc, and Kdn in this column were assigned to the same numbers/alphabets as in the first digit place (second column of the Table 1). We assigned leftover numbers to the naturally occurring monosaccharides such as galactose (Gal), *N*-acetylgalactosamine (GalNAc), and *N*-acetylglucosamine (GlcNAc). Apart from the listed ones, the occurrence of any other monosaccharides immediate to the terminal Sia is so far unknown. We did not use the numbers 3, 5, and 9 for the fourth digit place as there are no known linkages of non-terminal sialic acid through C-3, C-5, or C-9 positions (except on some bacterial capsular polysaccharide). Next, the branching at the second sugar unit was represented by the fifth digit. The branching monosaccharides were assigned along with their linkages. The Fuc α 1-2 (found in Lewis^Y, Lewis^B, and human blood group antigens); Gal α 1-3 (found in B-blood group antigen/ α -Gal), GalNAc β 1-4 (found in ganglio-series gangliosides), and 3/6-O-sulfation were assigned with the numbers that were in sync with the number assignments in other columns. Although we focused on trisaccharides, we took the liberty to accommodate some important natural glycans with longer side chains such as GM1 and Fuc-GM1 structures. The Gal β 1-3GalNAc β 1-4 and Fuc α 1-2Gal β 1-3GalNAc β 1-4 branches were assigned with letter *e* and *h* respectively. Next, the sixth digit was assigned to the linkage that connects the reducing end of the second sugar and the non-reducing end of the third sugar unit. The number assignment was in accordance with the previous linkage assignments listed in the fourth column (the third digit). The identity of the third sugar in the linear chain was denoted with the seventh digit. The number

assignment of the monosaccharide for the seventh digit place remained the same as in the second sugar unit (fourth digit). The only addition was the glucose (Glc) monosaccharide, which was assigned with number 5. The branching on the third sugar was designated in the eighth digit place in the coding system. The branched Sias on the third sugar were assigned with the numbers similar to those described for the first and the fourth digits. Again, the naturally occurring glycans and sulfated modifications were assigned with the numbers. In the eighth digit place, a series of di- and tri-saccharide branching (as found in Core 2, GD1) was considered and each was assigned with a letter. The linkage at the reducing end of the third sugar was designated in the ninth digit place. It is important to remember that the linkages had to be between two sugar units. Generally, the third sugar unit in our library was attached with an aliphatic linker at the reducing end and hence the ninth digit was always 0 (none) in our case. We assigned an additional tenth digit place to describe the linker connection or any further monosaccharides that are not present at this moment in our library. The α -linked linker was assigned with number 8 and β -linked linker is assigned with number 9. Utilizing the coding system, the sialoglycans in our library can be conveniently assigned with a 9-digit code (10-digit including the linker). Fig. 1 demonstrates the representation of sialoglycan in a machine-readable numerical format. See Supplementary data (Table SI) for the full list of the numerically encoded sialoglycans.

Application of the coding system for logical sorting of array results. One of the major reasons behind developing the coding system was to make the microarray data sorting easy and logical. Fig. 2 shows the binding of polyclonal chicken anti-Neu5Gc antibody (Diaz et al., 2009) on the sialoglycan microarray experiment. When the data were plotted against the semi-random glycan ID (Fig. 2A), the interpretation of data became clumsy and lacked a logical explanation. Once we applied the newly developed coding system on the glycans and sorted the data based on the 10-digit code, the chart became very clear and self-explanatory. The 10-digit codes were quickly arranged in an ascending order of the new encoded glycan ID (in Microsoft Excel) to logically group the Neu5Gc-glycans (and

its modified versions) together. The data plotted afterwards (as bar diagram) gave a clear visualization of the specificity of the antibody towards the Neu5Gc-epitopes (Fig. 2B).

In another example, we demonstrated that the 10-digit code not only can be helpful in arranging the data in ascending or descending order, but the numbers at the individual digit place can also be grouped together to convey a meaningful result. To demonstrate the technique, we tested the biotinylated *Sambucus nigra* lectin (SNA) on the sialoglycan microarray. The binding dataset was organized by grouping the linkages of the terminal Sia unit, i.e., the third digit. From the plot (Fig. 3), it was clearly demonstrated that SNA prefers to bind α 2-6-linked Sia epitopes.

Application of the coding system for motif searching of results. Among the versatile applications of the coding system, one important application was to search for the glycan motif responsible for binding to the lectins, proteins, and antibodies. Although our focus was on the terminal Sia, the underlying glycan structure plays a critical role that affects the binding pattern of the glycan-binding biomolecules. It is well-known that *Maackia amurensis* Lectin II (MAL II) recognizes the terminal Sia linked to the underlying glycan structures in α 2-3-linkage. The motif finding based on the new coding system also helped us to confirm the dependence of the binding specificity on the underlying glycan structures. We tested biotinylated MAL II on our sialoglycan microarray and a heat-map was plotted (Fig. 4). The top 20 strongest signals (average relative fluorescence unit, Ave RFU) obtained from the MAL II-binding on the microarray were listed along with the numerical code of the sialoglycan epitopes. It became obvious that all the strongly binding epitopes bore the same number sequence from third to seventh digit places, which eventually indicated that the Sia α 2-3 linked to the underlying Gal β 3GalNAc (sialyl T-antigen, an O-glycan) and Gal β 3GlcNAc (type 1) structures serve as the key motif for the MAL II binding. The coded number made the motif recognition much easier compared to finding the motif by reading the structures.

Coding-enabled enumeration of sialyltrisaccharide structures plausible and likely to appear in

nature. The systematic coding system also helped us calculate the number of possible sialyltrisaccharide structures that could exist in nature. In estimating the space of all, plausible and likely trisaccharides some fundamental concepts were applied. The set of *all* trisaccharides contains every trisaccharide code that can be written down. The set of *plausible* trisaccharides was extracted from that set by reasonably asserting that all sugars must be connected, and no modification or linkage can share a carbon; principles well established in glycobiology. Finally, the *likely* trisaccharides were extracted using a probabilistic approach to generalize glycan motifs found in a set of known trisaccharides. Here, we used co-occurrences observed between each adjacent and non-adjacent glycan element (sugar, linkage, and modification) to determine which two-element motifs were common, observed or never observed. Like the studies using motifs to generalize structural feasibility, the joint probabilities were aggregated over each novel trisaccharide to calculate a motif-based likelihood for each plausible trisaccharide. To enumerate all trisaccharide combinations and establish a total number for reference, we used a simple cartesian product; every selection of one element from each of several sets. Here, we enumerated every selection of one of the sugars, linkages, or modifications permissible at each of the 9 positions. The Cartesian product of the trisaccharide code gives 212,889,600 total trisaccharide combinations. To calculate the number of plausible trisaccharides, we selected from the set of all trisaccharides by asserting that trisaccharides must be connected and non-conflicting. Intuitively, no nonreducing sugar may follow a missing linkage (i.e., "None"). Similarly, no linkage or modification may connect to a missing reducing monosaccharide (i.e., "None"). Yet, a missing modification has no impact on the plausibility of the trisaccharide. We also applied constraints specifying the specific carbons each sugar provides for the formation of a glycosidic bond and the carbons required by a linkage or modification. Each monosaccharide provides a discrete number of hydroxyl groups at specific carbons, while each modification and linkage require a free hydroxyl group at specific carbons. In a plausible trisaccharide, each linkage and modification are associated with a sugar providing at least every necessary carbon to support those linkages and modifications. Additionally, the reducing linkage,

modification, and nonreducing linkage must not require the same carbons. After removing all unconnected trisaccharides (those with an interceding “None”), all conflicting trisaccharides (those with linkages and modifications requiring the same or unavailable carbons), there are 2,799,962, only 1.32% of the total, plausible trisaccharides remaining. Finally, we ranked the likelihood of trisaccharides by comparing them to a list of 140 known human trisaccharides. Because permissible reaction information is limited for trisaccharides, we used a statistical approach to infer feasible trisaccharide structures from the list of known human structures. We looked at the probability that any two elements in the trisaccharide code would co-occur in the set of 140 known sugars ($9 \text{ choose } 2 = 36$ pairs) and used that to generate a log-likelihood scoring. Due to the limited coverage of the combination space, we added a pseudo-count (0.1) to minimize the penalty of pairs unobserved in the known set. Over every plausible trisaccharide, the median log-likelihood was -21.7 and the median number of unobserved pairs per plausible trisaccharide was 6. The least likely trisaccharides have low log-likelihoods (min=-70.9) and high numbers of unobserved pairs (max=34). There were 113,781 trisaccharides with no unobserved pairs and these least unusual trisaccharides had a median log-likelihood of -8.07. There are 471,292 trisaccharides with at most 2 unobserved pairs and 746,861 trisaccharides with at most 3 unobserved pairs. With more unobserved pairs, the likelihood of that trisaccharide naturally occurring decreases.

In counting the total, plausible and likely trisaccharides, we found that these numbers differed by several orders of magnitude. The number of total trisaccharides is useful to orient us to the size of combinatorial possibility but has limited biological meaning as it contains many impossible structures with, for example, 1st and 3rd sugars with no 2nd sugar. The possible trisaccharide structures impose the minimal constraint, the sugar must be connected (no missing links or sugars) and all carbons requested by linkages or modifications must be requested only once and supported by the corresponding sugar. These constraints reduced the total sugar set from over 210 million to just over 2 million. The plausible sugars provide the most forgiving possible constraints and therefore describe an upper-bound suggesting that there are unlikely to be more than 2.8 million trisaccharides. Finally,

we imposed a harsh constraint, compliant with a set of known trisaccharides. 113,781 of the plausible trisaccharides were completely compliant with the set of known trisaccharides, containing no code pairs unobserved in the known set, suggesting that there are at least 113,781 sialyltrisaccharides. Though an unobserved pair makes it less likely that a trisaccharide is sterically feasible to assemble, the set of known trisaccharides was not comprehensive. Therefore, a trisaccharide with an unobserved pair may simply be a new type of trisaccharide. The more uncharacterized pairs a trisaccharide has, the less likely it is to contain no impossible code pairs. Therefore, a more forgiving lower-bound could be established as fewer than 2 or 3 unobserved pairs, 471,000 and 747,000 trisaccharides respectively. Within these large steps, trisaccharides can be ranked by log-likelihood to find the most likely sugars within each set. For the >113,000 plausible linear sialyltrisaccharides, we note that a biantennary *N*-glycan with two terminal sialoglycan trisaccharides could have $>10^{10}$ potential combinations and a triantennary *N*-glycan with three terminal sequences, $>10^{15}$ potential combinations at a single *N*-glycosylation site. With this calculation that includes selected sialic acid modifications and linkages, we greatly extended the possibility of 10,000 of *N*-glycans reported previously (Cummings, 2009).

Discovery of phylogenetically related bacterial AB₅ toxin B subunit from *Yersinia enterocolitica* (YenB) as a universal sialoglycan probe. The huge number of naturally possible sialyltrisaccharide structures, especially when branching is considered, poses an enormous challenge in probing of terminal Sia in a dynamic mammalian sialome (Srivastava et al., 2022). Traditional plant-based lectins are often limited in probing the sialosides due to the diverse and complex linkages and modification of terminal Sia. We addressed this challenge by exploiting the naturally-evolved sialic acid recognizing bacterial proteins which exhibit broad host range. Pathogen-glycan interactions are important both for colonization of host surfaces and recognition and entry of cells by toxins. A broad range of host compatibility (Wang et al., 2010) and phylogenetic proximity to the *Yersinia pestis* makes *Yersinia enterocolitica* a prime candidate that may express broad Sia recognizing proteins. Earlier studies

reported that plasmid-bearing *Y. enterocolitica* adhere to purified small intestinal mucins from rabbits and humans (Mantle and Husar, 1993; Mantle and Husar, 1994). The binding of the virulent bacteria with mucin was inhibited by purified mucin oligosaccharides and thus suggests the involvement of the glycan moiety in the cell specific interaction. Given the phylogenetic proximity of *Y. pestis* and *Y. enterocolitica* (Fig. 5) and the reported binding affinity of *Y. enterocolitica* with mucin carbohydrates, we anticipated that the *Y. enterocolitica* AB₅ toxin B subunit homologue YenB should recognize diverse Sia epitopes.

YenB (expressed with a C-terminal His6 tag) was purified from recombinant *E. coli* BL21, by Ni²⁺-NTA chromatography. The purified YenB protein was then tested for Sia binding using the sialoglycan microarray platform. Each glycan was printed in quadruplets on a *N*-hydroxysuccinimide coated glass slide and treated with the primary protein of optimized concentration. Average relative fluorescence unit (Ave RFU) was measured after treating with the Cy3-tagged secondary antibody. The sialoglycan coding system was used to rationally sort and plot the data for convenient interpretation. The microarray result (Fig. 6) demonstrated a broader Sia recognition by YenB compared to its phylogenetically-related homologue YpeB from *Y. pestis*. Interestingly, YenB showed a strong binding response against almost all types of Sia in our inventory including the 4-OAc, 5-OMe, and 8-OMe Sia, which YpeB failed to recognize. YenB bound to the Sia irrespective of the linkages (α 2-3; α 2-6; and α 2-8), modifications (4-OAc, 9-OAc, and 8-OMe), and underlying glycan structures (Fig.6). The only Neu5Gc-glycan that showed diminished binding was found to be Neu5Gc α 3Gal6S β 4(Fuc α 3)GlcNAc6S β R1. The presence of two sulfate groups probably interferes with the epitope recognition by YenB. Although YenB recognized the Neu5Ac and Neu5Gc-glycans promiscuously, it did not recognize Kdn-glycans. The lack of binding towards the non-sialosides confirmed that the binding of YenB is not promiscuous towards any glycan epitope.

Structure modeling study of YenB and development of YenB mutant for testing in the microarray: Since the crystal structure of YenB is not yet known, we constructed a structural model

of YenB using the crystal structure of SubB (3DWP) as a template. The structure model of YenB was achieved by aligning its primary amino acid sequence with other B pentamers and using crystal structure of SubB as template. The crystal structure of SubB was chosen as template because it shares the highest primary amino acid identity (57%) to YenB. Structural alignment of SubB with YenB (Fig. 7A), and YenB with YpeB (Fig. 7B) showed that YenB adopts the conserved OB fold which is typical of the B subunits from the AB₅ toxin family. With the available protein structure of SubB, it is known that serine residues are critical for binding to Neu5Ac, and tyrosine interacts with the extra hydroxyl group of Neu5Gc and are thus critical for binding to sialic acids (Byres et al., 2008). Upon aligning the sequences of *E. coli* SubB and *Y. enterocolitica* YenB (Fig. 8) we predicted that the mutation of conserved serine residue (S10) might adversely affect the glycan binding preferences. Additionally, the YenB binding site region has isoleucine (I82) as opposed to the conserved tyrosine (Y78) in the SubB (Fig. 9A). Notably, for YenB the residue adjacent to the I82 is a tyrosine (Y81), which is conserved in both species. To ensure a complete disruption of sialoglycan binding by the YenB, we mutated serine to alanine (S10A) and tyrosine to phenylalanine (Y81F) (Supplementary data Fig. S1). The recombinant YenB-mutant was expressed, and the protein was purified according to the similar method described for the YenB. The His-tagged YenB-mutant protein was tested on the microarray and no binding with the sialosides or the non-sialosides was observed whatsoever (Supplementary data Fig. S2).

Comparing the Neu5Gc-binding site of SubB with the proposed glycan-binding site within YenB reveals two major differences (Fig. 9A). Firstly, some of the critical SubB residues required for binding are not conserved suggesting that glycan binding is different. Secondly, the glycan-binding site in YenB is located below the position of glycan-binding site in SubB as binding residues in YenB are shifted down. Similar comparison to the YpeB glycan-binding site (Fig. 9B) also revealed a significant departure from the conservation of the amino acid residues at the binding site of YenB. Notably, the YenB has a tyrosine (Y8) residue near the C-4 position of the sialic acid whereas the YpeB and SubB

binding pockets have methionine residue (M30 and M10 respectively). This could be a possible reason for the differential 4-OAc sialoglycan binding preference between YenB versus YpeB and SubB.

Phylogenetic comparison of YenB with other AB₅ toxin B subunits (YpeB, SubB, PltB, ArtB, EcPltB, CtxB, and EcxB). The broad Sia binding propensity of YenB motivated us to explore other phylogenetically-related bacterial AB₅ toxin B subunits. We previously described the Sia-binding pattern of the Shiga toxogenic *E. coli* Subtilase cytotoxin B subunit (SubB), which shares 59% identity with YpeB (Khan et al., 2022). In addition, Sia-binding preferences of B subunits from closely related pathogenic *Salmonella enterica* serovars, *S. Typhi* (PltB) and *S. Typhimurium* (ArtB) were also tested on the sialoglycan microarray platform. Interestingly, a poor correlation was found between the phylogeny of known B subunit sequences in available genomes and bacterial species phylogeny (based on 16S rRNA). For example, based on B subunit phylogenetic tree inferences, YenB shares its clade with ArtB (54.24% sequence identity) but not with YpeB (Fig. 5).

Other than the aforementioned B subunits, we found three other closely related B subunits (Fig. 5), which might show interesting Sia-binding patterns. Some pathogenic extra-intestinal *E. coli* strains produce a pertussis-like AB₅ toxin (*EcPltAB*) (Littler et al., 2017), related to the toxins from typhoidal and nontyphoidal *Salmonella* serovars. *EcPltAB* toxin shares 70-80% sequence identity with *S. Typhi* PltAB. The B subunit of the toxin (*EcPltB*) also shares 69% sequence identity with ArtB from *S. Typhimurium*. A glycan array binding study of *EcPltB* displayed avidity for a broad range of branched eukaryotic glycans. However, the effect of modifications on the terminal Sia in *EcPltB* binding was less explored (Littler et al., 2017).

Cholera is a clinical-epidemiologic syndrome caused by *Vibrio cholerae* that induces severe and at times fatal diarrhea (Kaper et al., 1995), largely attributable to production of cholera toxin (CtxAB), the B subunit of which (CtxB) binds to gangliosides like GM1 (De Haan and Hirst, 2004). It has been reported that the Sia termini on the gangliosides play an important role in target cell recognition (Alisson-Silva et al., 2018), although there is also evidence for alternate fucose recognition (Cervin et al.,

2018; Wands et al., 2015) (which we did not study here). The cholera-like toxins are the largest subgroup of the B₅ toxin family. A novel cholera-like toxin was identified from a clinical isolate of *E. coli* (EcxAB) derived from diarrheal patients (Karasawa et al., 2002). Unlike other cholera-related AB₅ toxins, the unique mode of pairing of A subunit to the B subunit categorizes the EcxAB toxin in a novel AB₅ hybrid cholera-like toxin family. Although the A subunits EcxA and CtxA are structurally and functionally very distinct, the B subunits EcxB and CtxB share 63% sequence identity and almost complete structural homology (Ng et al., 2013). Like CtxB, EcxB was also reported to show strong binding preference towards Neu5Ac-associated ganglioside GM1 and fucosyl-GM1 structures (Ng et al., 2013). It was therefore of interest to determine whether the binding pattern changes upon substitution of Neu5Ac with Neu5Gc, a naturally less abundant variant which is not present in humans (Dhar et al., 2019).

Comparison of sialoglycan binding pattern of phylogenically-related B-subunits (YenB, YpeB, SubB, PltB, ArtB, EcPltB, CtxB, and EcxB). A diverse sialoglycan binding pattern emerged when the phylogenetically-related AB₅ toxin B subunits were tested on the microarray and the dataset was organized using the coding system. The comparative binding affinity of the phylogenetically-related six B subunits is presented in a standard heatmap format (Fig. 10). A common observation made for all the B subunits (except for EcxB) under consideration was that they did not show any propensity towards the non-sialosides present in our library (Supplementary data Fig. S3). Additionally, the B subunits failed to show any affinity towards glycans with a terminal Kdn (a rare mammalian Sia) (Kawanishi et al., 2021; Saha et al., 2021) unless there was an internal Neu5Ac/Gc present in the glycan structure (Supplementary data Fig. S3).

A broad range of Sia-binding by YenB protein has already been demonstrated (Fig. 6). Interestingly, YpeB, a closely related B-subunit protein showed versatile Sia recognition albeit lacking the ability to recognize 4-O-acetylated Sia (Fig. 10). The inability of YpeB to bind Neu4,5Ac₂ and Neu4Ac5Gc may hold the key to answering why some mammals (like horses) are thought to be less

susceptible to the plague. Neither of the B subunits could recognize the Kdn-glycans, except when the terminal Kdn is linked to an internal Neu5Ac or Neu5Gc in α 2-8 linkage.

A previous report of glycan microarray analysis of *E. coli* SubB showed a stronger binding preference towards the glycans terminating with α 2-3-linked Neu5Gc compared to its Neu5Ac congener (Byres et al., 2008). Testing of SubB in the expanded sialoglycan microarray revealed a similar binding pattern with a preferential α 2-3-linked Neu5Gc binding, irrespective of the underlying glycan structures. A weaker albeit significant binding was observed towards α 2-6 and α 2-8-linked Neu5Gc. The modification on Neu5Gc showed an immense effect in SubB binding. A moderately strong binding was observed towards the 9-OAc Neu5Gc-glycans, however the 5-OMe and 4-OAc modified Neu5Gc completely eliminated the affinity towards SubB. The loss of ligand ability of Neu5Gc upon 4-O-acetylation reaffirms the structural similarity of SubB to YpeB, which shares high sequence homology. Notably, Kdn associated glycans did not exhibit any binding to SubB.

Human specific typhoid toxin B subunit (PltB) binds exclusively with Neu5Ac-glycans (Deng et al., 2014). A detailed analysis of the binding preferences showed that the binding intensity decreases moderately when the terminal Neu5,9Ac₂ is linked to the underlying glycan in α 2-6 linkage. Interestingly, the binding was completely diminished when the terminal Neu5Ac was protected with an 8-OMe group.

An interesting observation was made when ArtB was tested on the microarray. Relative to PltB, ArtB showed a broader Sia preference with strong propensity towards α 2-3 and α 2-8-linked Neu5Ac- and acetylated Neu5Ac-glycans. However, terminal Neu5Ac with α 2-6-linkage exhibited 3 to 5-fold less binding intensity towards ArtB. Sialosides with terminal Neu5Gc showed a mild detrimental effect in binding with ArtB, which is unlike PltB where the Neu5Gc-glycan completely blocks Sia recognition.

EcPltB has been reported to preferably bind with Neu5Ac-glycans when tested at a higher concentration (100 μ g/ml) but partially loses its selectivity at low concentration (1 μ g/ml) (Littler et al., 2017). We tested the protein at 30 μ g/ml concentration and a mild preference towards Neu5Ac over Neu5Gc-glycans was observed. However, the Sia linkage plays an important role in binding affinity.

EcPitB showed a clear preference towards α 2-3 and α 2-8-linked Sia and failed to bind with α 2-6-linked Sia, a distinct trait that matches that seen in *ArtB*. Additionally, Sia recognition by *EcPitB* was completely blocked by 4-OAc modified Neu5Ac/Gc; a similar observation was made for *YpeB* and *SubB*.

The glycan recognition by *CtxB* and *EcxB* was very different when compared to other toxin B subunits under consideration. It is known that *CtxB* preferentially binds to naturally occurring GM1, where the Sia presented is Neu5Ac (De Haan and Hirst, 2004). When tested on the sialoglycan microarray we found that *CtxB* distinctly recognized both Neu5Ac- and Neu5Gc-associated GM1, as well as fucosylated-GM1. As expected, the binding intensity greatly diminished with GD1 as a ligand. No other sialosides and non-sialosides showed any affinity towards *CtxB*.

Like *CtxB*, *EcxB* also displayed a strong binding preference towards Neu5Ac- and Neu5Gc-GM1. It also recognized the fucosylated-GM1 glycan, albeit with relatively weaker affinity. Like in *CtxB*, GD1 was also found to be a moderately weak receptor for *EcxB*. The most striking differences in glycan binding between *CtxB* and *EcxB* was the recognition of non-sialosides. Notably, *EcxB* but not *CtxB* recognized the non-sialosides present in our library, which represented the terminal fragments of glycosphingolipids of either lacto, neo-lacto, or ganglio-series (Supplementary data Fig. S3). Fig. 10 heatmap shows a comparison of Sia-binding preferences.

Conclusions and Perspectives

Sialoglycan microarray analysis presents a great advantage in identifying novel interactions between sialoglycans and other biomolecules. We have established a chemoenzymatically synthesized defined sialyltrisaccharide library for the microarray technology platform. The challenges in sorting and finding motifs from vast microarray data were addressed by developing a novel 10-digit alpha-numerical coding system. The assignment of the code to the individual monosaccharide, their modification, and linkage made the analysis and visualization of data much easier and streamlined. This machine-readable code can be used to find binding target motifs. Using this coding system, we attempted to calculate the

number of plausible sialyltrisaccharide structures in nature. Our calculation revealed a remarkable number of at least 10^5 possible linear structures of sialyltrisaccharides and hence gave an idea of the huge structural diversity in whole sialomes where the structures of post-translational glycan modifications are not always linear. It is also evident that it is practically impossible to include all the possible natural sialyltrisaccharides on slide glycan array format.

This simple coding system brings value to the analysis of glycan array data, and does not require any special expertise, just standard spread-sheet software. Although the glycan coding is restricted in the number of saccharides it includes and lacks extensive branching, it can serve as a foundation to expand in future. This coding system for the sialyltrisaccharides can be easily expanded to the longer glycans and to non-sialosides. There is scope for scaling up with extended glycan array data, updating the set of rules, and automated data visualization. Based on the proposed coding system we established a rule-based approach that is interpretable and allows use by non-experts. While this could be further complemented with advanced machine learning methods (Bojar et al., 2021; Bao et al., 2021; Li et al., 2022) for identifying glycan motifs, the approach here provides a valuable and immediately interpretable framework. The system described here is by no means a perfect solution, yet an important step towards glycan array data management and natural glycan enumeration.

We evaluated the binding preferences of phylogenetically-related bacterial AB₅ toxin B subunits towards the sialoglycans using the sialoglycan microarray platform. We identified that the B subunit from *Y. enterocolitica* could recognize all Neu5Ac and Neu5Gc glycans present in our library irrespective of their modifications and linkages. This gives us an opportunity to use this toxin B subunit as a universal sialoglycan probe. We also re-evaluated the sialoside binding affinity of other phylogenetically-related B subunits. They presented a diverse array (Supplementary Data Table SII) of Sia-binding preferences, which can be exploited to develop a set of sialoglycan binding probes. We realize that it is impossible to have a microarray library that includes every possible naturally occurring sialoside. Moreover, the complexity of cell surface sialomes is beyond the scope of the defined

sialoglycan library. To probe the immense diversity of sialosides and dynamic changes of the sialome in biological models, we have proposed a set of Sialoglycan Recognition Probes (SGRP), to explore the (Srivastava et al., 2022).

UNCORRECTED MANUSCRIPT

Experimental Procedures

Enumeration and estimation of trisaccharides

In estimating the space of all plausible and likely trisaccharides some fundamental concepts were applied. The set of *all* trisaccharides contains every trisaccharide code that can be written down. The set of *plausible* trisaccharides was extracted from that set by reasonably asserting that all sugars must be connected, and no modification or linkage can share a carbon; principles well established in glycobiology. Finally, the *likely* trisaccharides were extracted using a probabilistic approach to generalize glycan motifs found in a set of known trisaccharides.

In a plausible trisaccharide, each linkage and modification are associated with a sugar providing at least every necessary carbon to support those linkages and modifications. Additionally, the reducing linkage, modification, and nonreducing linkage must not require the same carbons. Intuitively, no nonreducing sugar may follow a missing linkage (i.e., “None”). Similarly, no linkage or modification may connect to a missing reducing monosaccharide (i.e., “None”). Yet, a missing modification has no impact on the plausibility of the trisaccharide. We also applied constraints specifying the specific carbons each sugar provides for the formation of a glycosidic bond and the carbons required by a linkage or modification. Each monosaccharide provides a discrete number of hydroxyl groups at specific carbons, while each modification and linkage require a free hydroxyl group at specific carbons.

To calculate likely trisaccharides, we looked at the probability that any two elements in the trisaccharide code would co-occur in the set of 140 known sugars ($9 \text{ choose } 2 = 36$ pairs) and used that to generate a log-likelihood scoring. Due to the limited coverage of the combination space, we added a pseudo-count (0.1) to minimize the penalty of pairs unobserved in the known set.

Expression and purification of *Yersenia enterocolitica* B-subunit (YenB)

The method described in the reported literature (Khan et al., 2022) was followed to express and purify YenB protein with a C-terminal His₆ tag. The codon-optimized open reading frame encoding YenB was chemically synthesized, flanked by an *EcoRI* site and a ribosome binding site 5' to the initiating ATG

codon, and with a sequence encoding a His₆ tag fused to the C-terminus of the ORF and a 3' *Hind*III site, cloned into the respective sites of pUC57 (GenScript; Piscataway, NJ). The fragments were then excised and cloned into the *Eco*RI and *Hind*III sites of the expression vector pBAD18 (Guzman et al., 1995) such that the ORF is under the control of the vector *ara* promoter. This construct was then transformed into *E. coli* BL21.

For protein purification, the recombinant bacterium was grown in 500ml LB Broth supplemented with 50µg/ml ampicillin at 37°C to late logarithmic phase, diluted in half with fresh medium supplemented with 0.2% arabinose to induce *yenB* expression, and then incubated overnight at 26°C. Cells were harvested by centrifugation, resuspended in 20 ml loading buffer (50mM sodium phosphate, 300mM NaCl, 20 mM imidazole, pH 8.0), and lysed in a French pressure cell. Cell debris was removed by centrifugation at 20,000 × *g* for 30 min at 4°C. The supernatant was then loaded onto a 2ml column of Ni-nitrilotriacetic acid (NTA) resin, which had been preequilibrated with 20 ml loading buffer. The column was then washed with 40 ml loading buffer, and bound proteins were eluted with a 30-ml gradient of 0 to 500mM imidazole in loading buffer; 3ml fractions were collected and analyzed by SDS-PAGE, followed by staining with Coomassie blue or Western blotting with monoclonal anti-His₆. Fractions containing >95% pure YenB were pooled, concentrated, and stored in PBS/50% glycerol at -15°C.

Modeling study of YenB with sialosides

The YenB and other amino acid sequences were aligned using the program EXPRESSO (O'Sullivan et al., 2004), and homology modeling was performed employing MODELLER software (Eswar et al., 2006), using the crystal structure of SubB (3DWP) as a template.

Sialoglycan microarray

The sialoglycan microarray method was adapted and modified from the literature reported earlier (Meng et al., 2018; Lu et al., 2019). Defined sialosides with amine linker were chemoenzymatically synthesized

and then quantitated utilizing an improved DMB-HPLC method (Ji et al., 2021). 100 μ M of sialoglycan solution (in 300mM Na-phosphate buffer, pH 8.4) was printed in quadruplets on NHS-functionalized glass slides (PolyAn 3D-NHS; catalog# PO-10400401) using an ArrayIt SpotBot® Extreme instrument. The slides were blocked (0.05M ethanolamine solution in 0.1M Tris-HCl, pH 9.0), washed with warm Milli-Q water and dried.

The slides were then fitted in a multi-well microarray hybridization cassette (ArrayIt, CA) to divide into 8 wells and rehydrated with 400 μ l of Ovalbumin (1% w/v, PBS) for one hour in a humid chamber with gentle shaking. After that the blocking solution was discarded and a 400 μ l of solution of the toxin B-subunit (30 μ g/ml) in the same blocking buffer was added to the individual well. The slides were incubated for 2h at room temperature with gentle shaking and the slides were washed with PBS-Tween (0.1% v/v). The wells were then treated with Cy3-conjugated anti-His (Rockland Antibodies & Assays; Cat# 200-304-382) secondary antibody at 1:500 dilution in PBS. Followed by gentle shaking for 1 hour in the dark and humid chamber. The slides were then washed, dried, and scanned with a Genepix 4000B scanner (Molecular Devices Corp., Union City, CA) at wavelength 532 nm. Data analysis was performed using the Genepix Pro 7.3 software (Molecular Devices Corp., Union City, CA). The raw data analysis and sorting using the numerical codes were performed on Microsoft Excel.

Data availability

All data are contained within the main text and supporting information.

Acknowledgments

This work was supported by NIH Grant R01GM32373 (to A.V.), the Novo Nordisk Foundation (NNF10CC1016517, NNF20SA0066621), and NIGMS R35GM119850 (to N.E.L.).

Conflicts of Interest

The authors declare no competing financial interests.

References

- Akune, Y, et al. (2022), 'CarbArrayART: a new software tool for carbohydrate microarray data storage, processing, presentation, and reporting.', *Glycobiology*, 32 (7), 552-55.
- Alisson-Silva, F, et al. (2018), 'Human evolutionary loss of epithelial Neu5Gc expression and species-specific susceptibility to cholera.', *PLoS Pathog*, 14 (6), e1007133.
- Banin, Ehud, et al. (2002), 'A novel linear code® nomenclature for complex carbohydrates', *Trends in Glycoscience and Glycotechnology*, 14 (77), 127-37.
- Bao, B, et al. (2021), 'Correcting for sparsity and interdependence in glycomics by accounting for glycan biosynthesis.', *Nat Commun*, 12 (1), 4988.
- Benedetti, E, et al. (2017), 'Network inference from glycoproteomics data reveals new reactions in the IgG glycosylation pathway.', *Nat Commun*, 8 (1), 1483.
- Bensing, BA, et al. (2016), 'Novel aspects of sialoglycan recognition by the Siglec-like domains of streptococcal SRR glycoproteins.', *Glycobiology*, 26 (11), 1222-34.
- Black, RE, et al. (1978), 'Epidemic *Yersinia enterocolitica* infection due to contaminated chocolate milk.', *N Engl J Med*, 298 (2), 76-79.
- Bohne-Lang, A, et al. (2001), 'LINUCS: linear notation for unique description of carbohydrate sequences.', *Carbohydr Res*, 336 (1), 1-11.
- Bojar, D, et al. (2021), 'Deep-Learning Resources for Studying Glycan-Mediated Host-Microbe Interactions.', *Cell Host Microbe*, 29 (1), 132-144.e3.
- Byres, E, et al. (2008), 'Incorporation of a non-human glycan mediates human susceptibility to a bacterial toxin.', *Nature*, 456 (7222), 648-52.
- Cao, Y, et al. (2020), 'GlyMDB: Glycan Microarray Database and analysis toolset.', *Bioinformatics*, 36 (8), 2438-42.
- Cervin, J, et al. (2018), 'GM1 ganglioside-independent intoxication by Cholera toxin.', *PLoS Pathog*, 14 (2), e1006862.
- Chen, X and A Varki (2010), 'Advances in the biology and chemistry of sialic acids.', *ACS Chem Biol*, 5 (2), 163-76.
- Cholleti, SR, et al. (2012), 'Automated motif discovery from glycan array data.', *OMICS*, 16 (10), 497-512.
- Coff, Lachlan, et al. (2020), 'Identifying glycan motifs using a novel subtree mining approach', *BMC bioinformatics*, 21 (1), 42.
- Cummings, RD (2009), 'The repertoire of glycan determinants in the human glycome.', *Mol Biosyst*, 5 (10), 1087-104.
- De Haan, L and TR Hirst (2004), 'Cholera toxin: a paradigm for multi-functional engagement of cellular mechanisms (Review).', *Mol Membr Biol*, 21 (2), 77-92.
- Deng, L, X Chen, and A Varki (2013), 'Exploration of sialic acid diversity and biology using sialoglycan microarrays.', *Biopolymers*, 99 (10), 650-65.
- Deng, L, et al. (2014), 'Host adaptation of a bacterial toxin from the human pathogen *Salmonella Typhi*.', *Cell*, 159 (6), 1290-99.
- Dhar, C, A Sasmal, and A Varki (2019), 'From "Serum Sickness" to "Xenosialitis": Past, Present, and Future Significance of the Non-human Sialic Acid Neu5Gc.', *Front Immunol*, 10 807.
- Dhar, C, et al. (2021), 'Are sialic acids involved in COVID-19 pathogenesis', *Glycobiology*, 31 (9), 1068-71.
- Diaz, SL, et al. (2009), 'Sensitive and specific detection of the non-human sialic Acid N-glycolylneuraminic acid in human tissues and biotherapeutic products.', *PLoS One*, 4 (1), e4241.
- Doubet, S, et al. (1989), 'The Complex Carbohydrate Structure Database.', *Trends Biochem Sci*, 14 (12), 475-77.
- Doubet, S and P Albersheim (1992), 'CarbBank.', *Glycobiology*, 2 (6), 505.
- Eswar, N, et al. (2006), 'Comparative protein structure modeling using Modeller.', *Curr Protoc Bioinformatics*, Chapter 5 Unit-5.6.
- Guzman, LM, et al. (1995), 'Tight regulation, modulation, and high-level expression by vectors containing the arabinose PBAD promoter.', *J Bacteriol*, 177 (14), 4121-30.

- Hashimoto, K, et al. (2005), 'KEGG as a glycome informatics resource.', *Glycobiology*,
- Hosoda, M, et al. (2018), 'MCAW-DB: A glycan profile database capturing the ambiguity of glycan recognition patterns.', *Carbohydr Res*, 464 44-56.
- Ji, Y, et al. (2021), 'Reversible O-Acetyl Migration within the Sialic Acid Side Chain and Its Influence on Protein Recognition.', *ACS Chem Biol*, 16 (10), 1951-60.
- Kaper, JB, JG Morris, and MM Levine (1995), 'Cholera.', *Clin Microbiol Rev*, 8 (1), 48-86.
- Karasawa, T, et al. (2002), 'Cloning and characterization of genes encoding homologues of the B subunit of cholera toxin and the Escherichia coli heat-labile enterotoxin from clinical isolates of Citrobacter freundii and E. coli.', *Infect Immun*, 70 (12), 7153-55.
- Kawanishi, K, et al. (2021), 'Evolutionary conservation of human ketodeoxynonulosonic acid production is independent of sialoglycan biosynthesis.', *J Clin Invest*, 131 (5), 137681.
- Kay, BA, et al. (1983), 'Virulence and phenotypic characterization of Yersinia enterocolitica isolated from humans in the United States.', *J Clin Microbiol*, 17 (1), 128-38.
- Kellman, BP, et al. (2020), 'A consensus-based and readable extension of Linear Code for Reaction Rules (LiCoRR).', *Beilstein J Org Chem*, 16 2645-62.
- Kellman, BP and NE Lewis (2021), 'Big-Data Glycomics: Tools to Connect Glycan Biosynthesis to Extracellular Communication.', *Trends Biochem Sci*, 46 (4), 284-300.
- Khan, N, et al. (2022), 'Sialoglycan-binding patterns of bacterial AB₅ toxin B subunits correlate with host range and toxicity, indicating evolution independent of A subunits.', *J Biol Chem*, 298 (5), 101900.
- Kikuchi, N, et al. (2005), 'The carbohydrate sequence markup language (CabosML): an XML description of carbohydrate structures.', *Bioinformatics*, 21 (8), 1717-18.
- Klamer, Z, et al. (2017), 'Mining High-Complexity Motifs in Glycans: A New Language To Uncover the Fine Specificities of Lectins and Glycosidases.', *Anal Chem*, 89 (22), 12342-50.
- Klamer, Z, et al. (2019), 'Deciphering Protein Glycosylation by Computational Integration of On-chip Profiling, Glycan-array Data, and Mass Spectrometry.', *Mol Cell Proteomics*, 18 (1), 28-40.
- Klein, J and J Zaia (2019), 'glypy: An Open Source Glycoinformatics Library.', *J Proteome Res*, 18 (9), 3532-37.
- Laine, RA (1994), 'A calculation of all possible oligosaccharide isomers both branched and linear yields 1.05 x 10¹² structures for a reducing hexasaccharide: the Isomer Barrier to development of single-method saccharide sequencing or synthesis systems.', *Glycobiology*, 4 (6), 759-67.
- Lewis, AL, et al. (2022), 'Sialic Acids and Other Nonulosonic Acids', in Varki, A, et al. (eds.), *Essentials of Glycobiology* (Cold Spring Harbor (NY): Cold Spring Harbor Laboratory Press),
- Li, H, AWT Chiang, and NE Lewis (2022), 'Artificial intelligence in the analysis of glycosylation data.', *Biotechnol Adv*, 60 108008.
- Littler, DR, et al. (2017), 'Structure-function analyses of a pertussis-like toxin from pathogenic Escherichia coli reveal a distinct mechanism of inhibition of trimeric G-proteins.', *J Biol Chem*, 292 (36), 15143-58.
- Lu, N, et al. (2019), 'Redox-Controlled Site-Specific α -2-6-Sialylation.', *J Am Chem Soc*, 141 (11), 4547-52.
- Mantle, M and SD Husar (1993), 'Adhesion of Yersinia enterocolitica to purified rabbit and human intestinal mucin.', *Infect Immun*, 61 (6), 2340-46.
- Mantle, M and SD Husar (1994), 'Binding of Yersinia enterocolitica to purified, native small intestinal mucins from rabbits and humans involves interactions with the mucin carbohydrate moiety.', *Infect Immun*, 62 (4), 1219-27.
- McNaught, AD (1997), 'International Union of Pure and Applied Chemistry and International Union of Biochemistry and Molecular Biology. Joint Commission on Biochemical Nomenclature. Nomenclature of carbohydrates.', *Carbohydr Res*, 297 (1), 1-92.
- Mehta, AY, J Heimburg-Molinaro, and RD Cummings (2020), 'Tools for generating and analyzing glycan microarray data.', *Beilstein J Org Chem*, 16 2260-71.
- Meng, C, et al. (2018), 'Chemoenzymatic Assembly of Mammalian O-Mannose Glycans.', *Angew Chem Int Ed Engl*, 57 (29), 9003-7.
- Ng, NM, et al. (2013), 'EcxAB is a founding member of a new family of metalloprotease AB₅ toxins with a hybrid cholera-like B subunit.', *Structure*, 21 (11), 2003-13.

- O'Loughlin, EV, DG Gall, and CH Pai (1990), 'Yersinia enterocolitica: mechanisms of microbial pathogenesis and pathophysiology of diarrhoea.', *J Gastroenterol Hepatol*, 5 (2), 173-79.
- O'Sullivan, O, et al. (2004), '3DCoffee: combining protein sequences and structures within multiple sequence alignments.', *J Mol Biol*, 340 (2), 385-95.
- Otsubo, N, et al. (2001), 'The first, efficient synthesis of novel sLex neoglycolipids containing N-deacetylated and lactamized sialic acid: Key ligand structures for selectin binding', *J Carbohydr Chem*, 20 329-34.
- Padler-Karavani, V, et al. (2012), 'Cross-comparison of protein recognition of sialic acid diversity on two novel sialoglycan microarrays.', *J Biol Chem*, 287 (27), 22593-608.
- Pérez, S and B Mulloy (2005), 'Prospects for glycoinformatics.', *Curr Opin Struct Biol*, 15 (5), 517-24.
- Raman, R, et al. (2006), 'Advancing glycomics: implementation strategies at the consortium for functional glycomics.', *Glycobiology*, 16 (5), 82R-90R.
- Saha, S, et al. (2021), 'Exploring the Impact of Ketodeoxynonulosonic Acid in Host-Pathogen Interactions Using Uptake and Surface Display by Nontypeable Haemophilus influenzae.', *mBio*, 12 (1), e03226-20.
- Sahoo, SS, et al. (2005), 'GLYDE-an expressive XML standard for the representation of glycan structure.', *Carbohydr Res*, 340 (18), 2802-7.
- Shinmachi, Daisuke, et al. (2017), 'Using GlyTouCan Version 1.0: The First International Glycan Structure Repository', *A Practical Guide to Using Glycomics Databases* (Springer), 41-73.
- Srivastava, S, et al. (2022), 'Development and applications of sialoglycan-recognizing probes (SGRPs) with defined specificities: exploring the dynamic mammalian sialoglycome.', *Glycobiology*, cwac050.
- Tang, H, et al. (2015), 'The detection and discovery of glycan motifs in biological samples using lectins and antibodies: new methods and opportunities.', *Adv Cancer Res*, 126 167-202.
- Tiemeyer, M, et al. (2017), 'GlyTouCan: an accessible glycan structure repository.', *Glycobiology*, 27 (10), 915-19.
- Toma, S and L Lafleur (1974), 'Survey on the incidence of Yersinia enterocolitica infection in Canada.', *Appl Microbiol*, 28 (3), 469-73.
- Toukach, P, et al. (2007), 'Sharing of worldwide distributed carbohydrate-related digital resources: online connection of the Bacterial Carbohydrate Structure DataBase and GLYCOSCIENCES.de.', *Nucleic Acids Res*, 35 (Database issue), D280-6.
- Varki, A and T Angata (2006), 'Siglecs--the major subfamily of I-type lectins.', *Glycobiology*, 16 (1), 1R-27R.
- Varki, A, et al. (2015), 'Symbol Nomenclature for Graphical Representations of Glycans.', *Glycobiology*, 25 (12), 1323-24.
- Venkataraman, M, R Sasisekharan, and R Raman (2015), 'Glycan array data management at Consortium for Functional Glycomics.', *Methods Mol Biol*, 1273 181-90.
- Von der Lieth, CW, et al. (2004), 'Bioinformatics for glycomics: status, methods, requirements and perspectives.', *Brief Bioinform*, 5 (2), 164-78.
- von der Lieth, Claus-W (2004), 'An endorsement to create open access databases for analytical data of complex carbohydrates', *Journal of carbohydrate chemistry*, 23 (5), 277-97.
- Wands, AM, et al. (2015), 'Fucosylation and protein glycosylation create functional receptors for cholera toxin.', *Elife*, 4 e09545.
- Wang, X, et al. (2010), 'Pathogenic strains of Yersinia enterocolitica isolated from domestic dogs (Canis familiaris) belonging to farmers are of the same subtype as pathogenic Y. enterocolitica strains isolated from humans and may be a source of human infection in Jiangsu Province, China.', *J Clin Microbiol*, 48 (5), 1604-10.
- Yamaguchi, M, et al. (2003), 'Studies on the endogenous L-selectin ligands: systematic and highly efficient total synthetic routes to lactamized-sialyl 6-O-sulfo Lewis X and other novel gangliosides containing lactamized neuraminic acid.', *Carbohydr Res*, 338 (24), 2793-812.
- Ye, Jinfeng, et al. (2016), 'Diversity-Oriented Enzymatic Modular Assembly of ABO Histo-blood Group Antigens', *ACS Catal*, 6 (12), 8140-44.
- Yusufi, FN, et al. (2009), 'An alpha-numeric code for representing N-linked glycan structures in secreted glycoproteins.', *Bioprocess Biosyst Eng*, 32 (1), 97-107.

Figure Legends

Figure 1: Coding strategy utilized to encode sialyltrisaccharides. Codes associated with the individual glycan identity, modification, and linkage are listed starting from the non-reducing end. Example of 10-digit numerical code representation of sialyltrisaccharides. New glycan id (extreme right column) is generated based on the encoding rules described in Table I. The left most column describes the semi random old glycan id which is based on the order of which the glycans were synthesized and stored. For complete list see Table SI (Supplementary Data).

Figure 2: Application of coding system to identify binding patterns. Chicken polyclonal anti-Neu5Gc IgY antibody was tested on sialoglycan microarray platform and average fluorescence unit (Ave RFU) was plotted against a) semi-random glycan id and b) new glycan code arranged according to the terminal Sia identity. The lone strong signal at the left of the plot corresponds to the glycan Neu5Ac α 6(Neu5Gc α 3)Gal β 4Glc β R1.

Figure 3: Application of coding system for logical sorting of microarray data. The data obtained from the microarray experiment with biotinylated SNA lectin was organized based on the linkage between the terminal Sia and the underlying glycan structure. The plot conveniently and clearly shows the preference of SNA lectin towards the α 2-6-linked Sia.

Figure 4: Motif finding utilizing the new sialoglycan code. Top 20 strongest signal obtained from sialoglycan microarray experiment of Biotinylated *Maackia Amurensis* Lectin II (MAL II) was listed along with the 10-digit new glycan id. The digits labelled in red showing a clear motif in glycan structure that serves as the ligand epitope of MAL II. The most prominent motifs determined here are the Sia α 3Gal β 3GalNAc α (O-glycans) along with the Sia α 3Gal β 3GlcNAc (type 1) structures.

Figure 5: Phylogenetic relationship between species based on 16S rRNA vs pentavalent B subunit of exotoxins. The comparison reveals that the evolution of bacterial AB₅ toxin B subunit is independent of the species phylogeny. Corresponding accession numbers are indicated below.

Figure 6: Sialoglycan microarray experiment with B subunit from *Y. enterocolitica*. The chart showed broad range sialic acid recognition by the His-tagged YenB protein (30 μ g/ml). The glycans on the X-axis is in the order as listed in the Table SI (supplementary data). The non-sialoside and Kdn-glycan epitopes were not recognized by the YenB. Ganglioside type glycan epitopes are designated as

asterisk symbol (*) in the chart. Error bar represents the standard deviation for each glycan printed in quadruplicate.

Figure 7: YenB structure modelling and comparison with SubB and YpeB. A) Superposition of the SubB X-ray structure (pale pink) (PDB code:3DWP) with model of YenB (cyan). Overall, very similar to SubB, YenB has longer helix at a distance from the binding site (showed by arrows). B) Superposition of the YpeB (pale green) and YenB (cyan) 3-dimensional model. The structure models are very similar to each other except a few longer helices at a distance from the binding site (showed by arrows).

Figure 8: Alignment of the sequence for the B subunits from the *Y. enterocolitica* (YenB) and *E. coli* (SubB). The conserved serine residue is highlighted in red.

Figure 9: Interaction of sialic acid (Neu5Gc) at the binding pocket of YenB and others. A) Superposition of the Neu5Gc binding site of SubB (pale pink) with the model of YenB (cyan) using the C-alpha coordinates of all residues. Neu5Gc is highlighted in light purple. B) Superposition of the Neu5Gc (light purple) binding site of SubB (pink) with the model of YpeB (pale green) and model of YenB (cyan) using the C-alpha coordinates of all residues. Neu5Gc is highlighted in light purple.

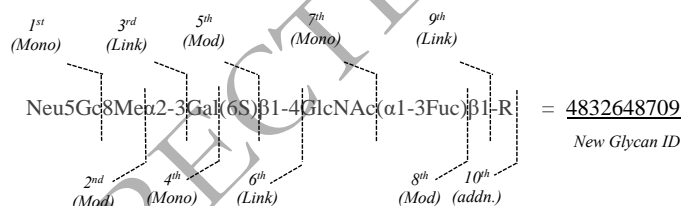
Figure 10: Differential sialoglycan recognition by phylogenetically-related toxin B subunits. Data obtained from sialoglycan microarray experiment showed a diverse Sia binding affinity. The glycan structures were grouped according to the terminal Sia, modifications, and linkages to identify the binding pattern of various phylogenetically-related B subunits. [see supp. Info. section for the Ave RFU numerical data. For a qualitative binding comparison see Supplementary data Table SII].

Table I: Numerical code for designating naturally occurring trisaccharide sequences carrying terminal sialic acids. In first digit place alphabetical codes are used for less common or bacterial terminal glycan sequences carrying nonulosonic acid units.

Code	1 st Terminal Sia/NuIO	2 nd Mod.	3 rd Link	4 th Second Sugar	5 th Mod/ Branch	6 th Link	7 th Third sugar	8 th Mod/ Branch	9 th Link	10 th Additional
1	Neu5Ac	1,7 Lactone		Neu5Ac	Fucα1-2	α1-3	Neu5Ac	(Neu5Acα2-6)	α1-3	Gal
2	Neu4,5Ac ₂	(8OS)		Gal	Galα1-3	β1-3	Gal	(GalNAcβ1-4)	β1-3	Glcβ1
3	Neu5,9Ac ₂	9-O-Lactyl	α2-3		(3OS)	α2-3		(GlcNAcβ1-6)	α2-3	GlcNAcβ1
4	Neu5Gc	4,9-di-OAc	α2-4	Neu5Gc	(GalNAcβ1-4)	β1-4	Neu5Gc	(Neu5Gcα2-6)	β1-4	Man
5	Neu4Ac5Gc	5-OMe	α2-5				Glc	(Fucα1-4)	β1-2	
6	Neu5Gc9Ac	7,8,9-triOAc	α2-6	GalNAc	(6OS)	α2-6	GalNAc	(6OS)	α2-6	Galβ1-4Glcβ1
7	Kdn	7-OAc	α2-7	Kdn			Kdn	(Fucα1-3)	β1-6	Galβ1-4GlcNAc
8	Kdn4Ac	8-OMe	α2-8	GlcNAc		α2-8	GlcNAc	(6OS, Fucα1-3)	α2-8	α1-1' (with linker)
9	Kdn9Ac	(7/8)9-diOAc	α2-9			α2-9		(6OS, Fucα1-4)		β1-1' (with linker)
0	None	None	None	None	None	None	None	None	None	
a	Neu	1,5 Lactam		Neu	(Neu5Acα2-3-)		Neu	(Galβ1-4GlcNAcβ1-6)		
b	Leg				(Neu5Gcα2-3-)			(Neu5Acα2-3Galβ1-4GlcNAcβ1-6)		
c	Leg5,7Ac ₂				(Kdnα2-3-)			(Neu5Acα2-6Galβ1-4GlcNAcβ1-6)		
d	Pse									
e	Aci				(Galβ1-3GalNAcβ1-4)			(Galβ1-3GalNAcβ1-4)		
f	4eLeg5,7Ac ₂				(Neu5Acα2-3Galβ1-3GalNAcβ1-4)			(Neu5Acα2-3Galβ1-3GalNAcβ1-4)		
g	8eLeg5,7Ac ₂				(Neu5Acα2-6Galβ1-3GalNAcβ1-4)			(Neu5Acα2-6Galβ1-3GalNAcβ1-4)		
h					(Fucα1-2Galβ1-3GalNAcβ1-4)			(Fucα1-2Galβ1-3GalNAcβ1-4)		

Figures

Fig. 1



Glycan ID	Glycan Structure	1st	2nd	3rd	4th	5th	6th	7th	8th	9th	10th	New Glycan ID
1	Neu5,9Ac2α3Galβ4GlcNAcβR1	3	0	3	2	0	4	8	0	0	9	3032048009
2	Neu5Gc9Acα3Galβ4GlcNAcβR1	6	0	3	2	0	4	8	0	0	9	6032048009
3	Neu5,9Ac2α6Galβ4GlcNAcβR1	3	0	6	2	0	4	8	0	0	9	3062048009
4	Neu5Gc9Acα6Galβ4GlcNAcβR1	6	0	6	2	0	4	8	0	0	9	6062048009
5	Neu5Acα6GalNAcαR1	1	0	6	6	0	0	0	0	0	8	1066000008
6	Neu5Gcα6GalNAcαR1	4	0	6	6	0	0	0	0	0	8	4066000008
7	Neu5,9Ac2α3Galβ3GlcNAcβR1	3	0	3	2	0	2	8	0	0	9	3032028009
8	Neu5Gc9Acα3Galβ3GlcNAcβR1	6	0	3	2	0	2	8	0	0	9	6032028009
9	Neu5,9Ac2α3Galβ3GalNAcαR1	3	0	3	2	0	2	6	0	0	8	3032026008
10	Neu5Gc9Acα3Galβ3GalNAcαR1	6	0	3	2	0	2	6	0	0	8	6032026008

Fig. 2

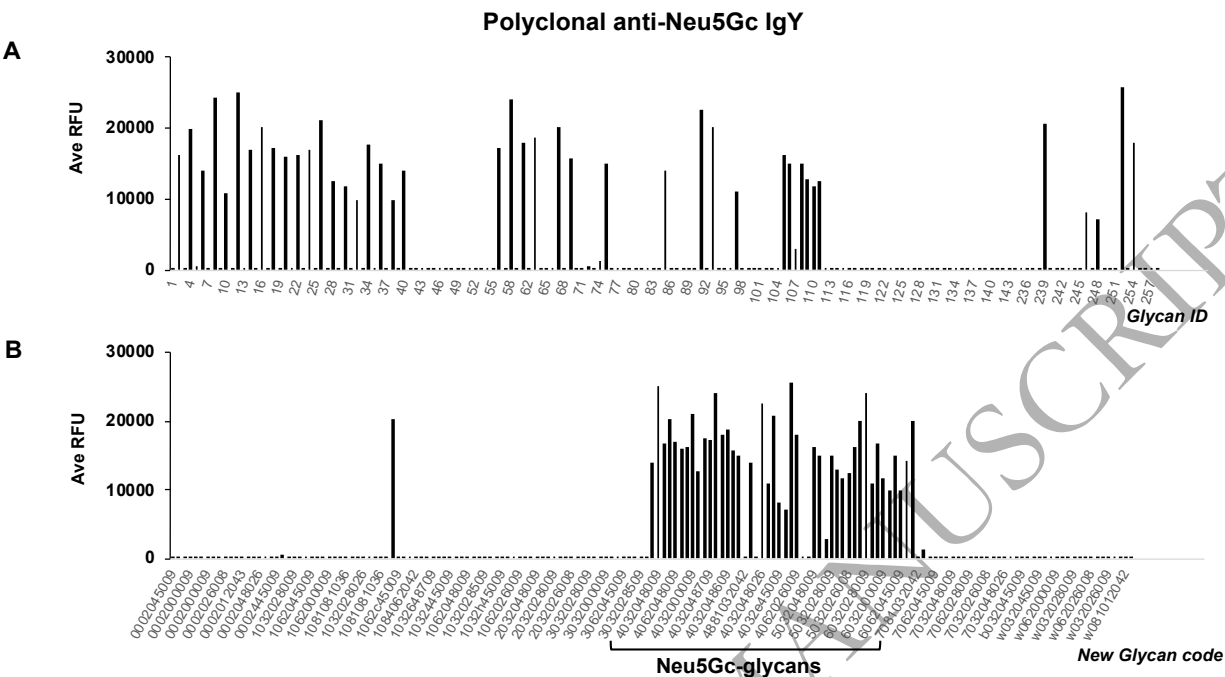


Fig. 3

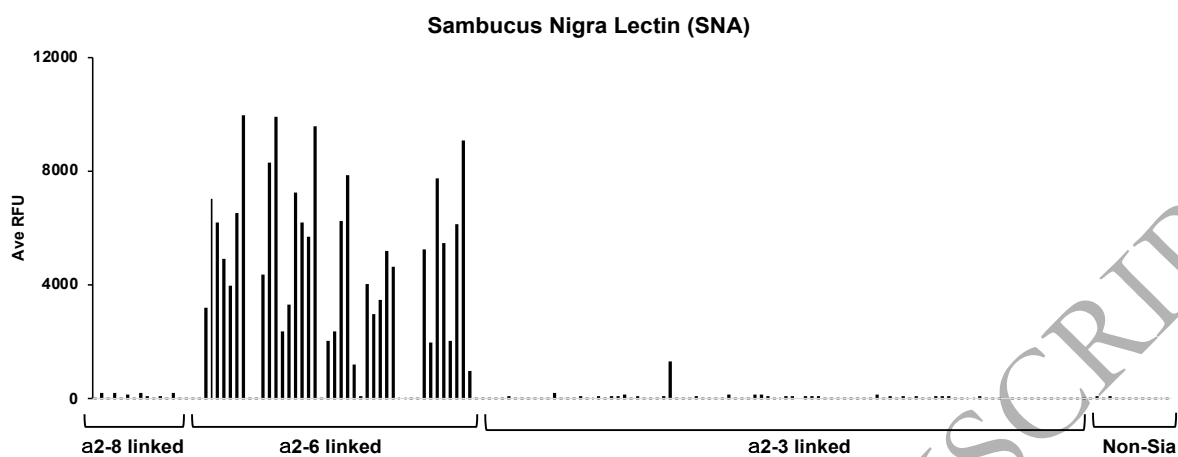


Fig. 4

Glycan Structure	1st	2nd	3rd	4th	5th	6th	7th	8th	9th	10th	New Glycan ID	Ave RFU
Neu5Gca3Galβ3GalNAcaR1	4	0	3	2	0	2	6	0	0	8	40 32026 008	
Neu5,9Ac2α3Galβ3GalNAcaR1	3	0	3	2	0	2	6	0	0	8	30 32026 008	
Neu5Acα3Galβ3GalNAcaR1	1	0	3	2	0	2	6	0	0	8	10 32026 008	
Neu4Ac5Gca3Galβ3GalNAcaR1	5	0	3	2	0	2	6	0	0	8	50 32026 008	
Neu5Acα3Galβ3GalNAcβR1	1	0	3	2	0	2	6	0	0	9	10 32026 009	
Neu4Ac5Gca3Galβ3GlcNAcaR1	5	0	3	2	0	2	8	0	0	8	50 32028 008	
Neu5Gca3Galβ3GalNAcβR1	4	0	3	2	0	2	6	0	0	9	40 32026 009	
Neu4,5Ac2α3Galβ3GalNAcaR1	2	0	3	2	0	2	6	0	0	8	20 32026 008	
Neu4,5Ac2α3Galβ3GalNAcβR1	2	0	3	2	0	2	6	0	0	9	20 32026 009	
Neu4Ac5Gca3Galβ3GalNAcβR1	5	0	3	2	0	2	6	0	0	9	50 32026 009	
Neu4,5Ac2α3Galβ3GlcNAcβR1	2	0	3	2	0	2	8	0	0	9	20 32028 009	
Neu4,5Ac2α-3Galβ3GlcNAcaR1	2	0	3	2	0	2	8	0	0	8	20 32028 008	
Neu5Gc9Acα3Galβ3GalNAcaR1	6	0	3	2	0	2	6	0	0	8	60 32026 008	
Neu5Acα3Galβ3GlcNAcaR1	1	0	3	2	0	2	8	0	0	8	10 32028 008	
Neu4Ac5Gca3Galβ3GlcNAcβR1	5	0	3	2	0	2	8	0	0	9	50 32028 009	
Neu5,9Ac2α3Galβ3GalNAcβR1	3	0	3	2	0	2	6	0	0	9	30 32026 009	
Neu5Gc9Acα3Galβ3GalNAcβR1	6	0	3	2	0	2	6	0	0	9	60 32026 009	
Neu5Gca3Galβ3GlcNAcβR1	4	0	3	2	0	2	8	0	0	9	40 32028 009	
Neu5Acα3Galβ3GlcNAcβR1	1	0	3	2	0	2	8	0	0	9	10 32028 009	

Fig. 5

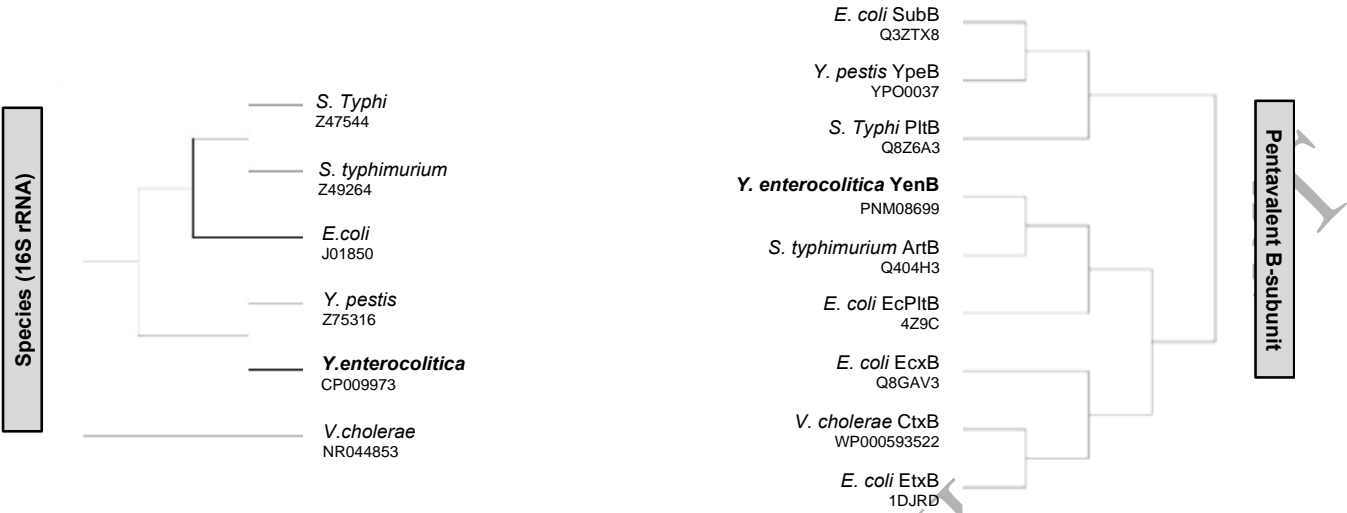


Fig. 6

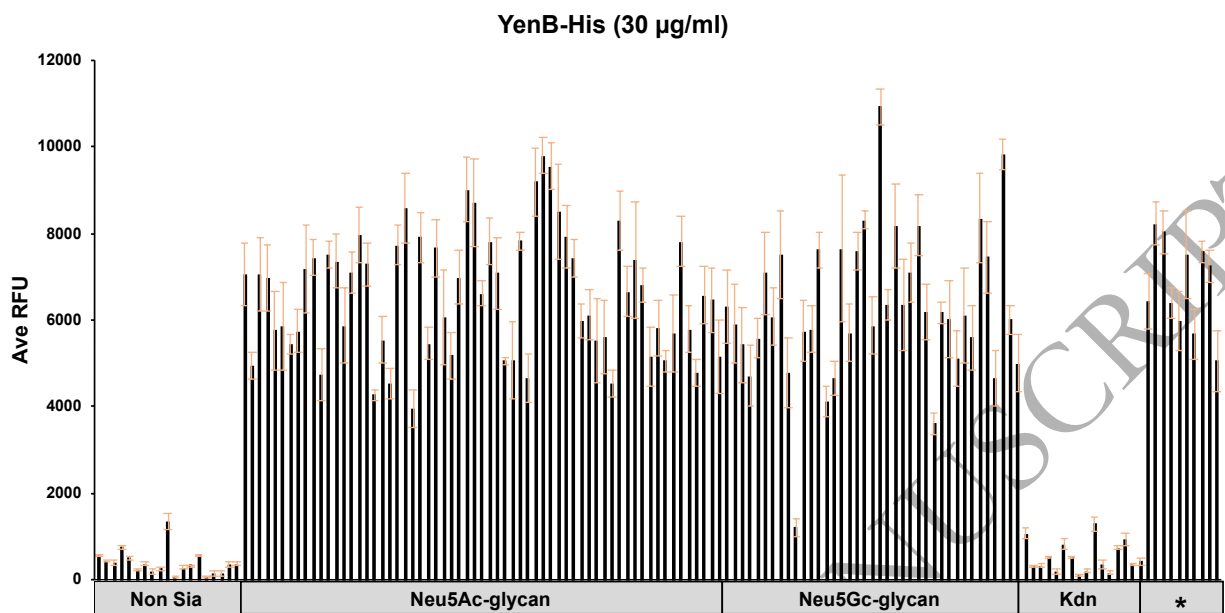


Fig. 7

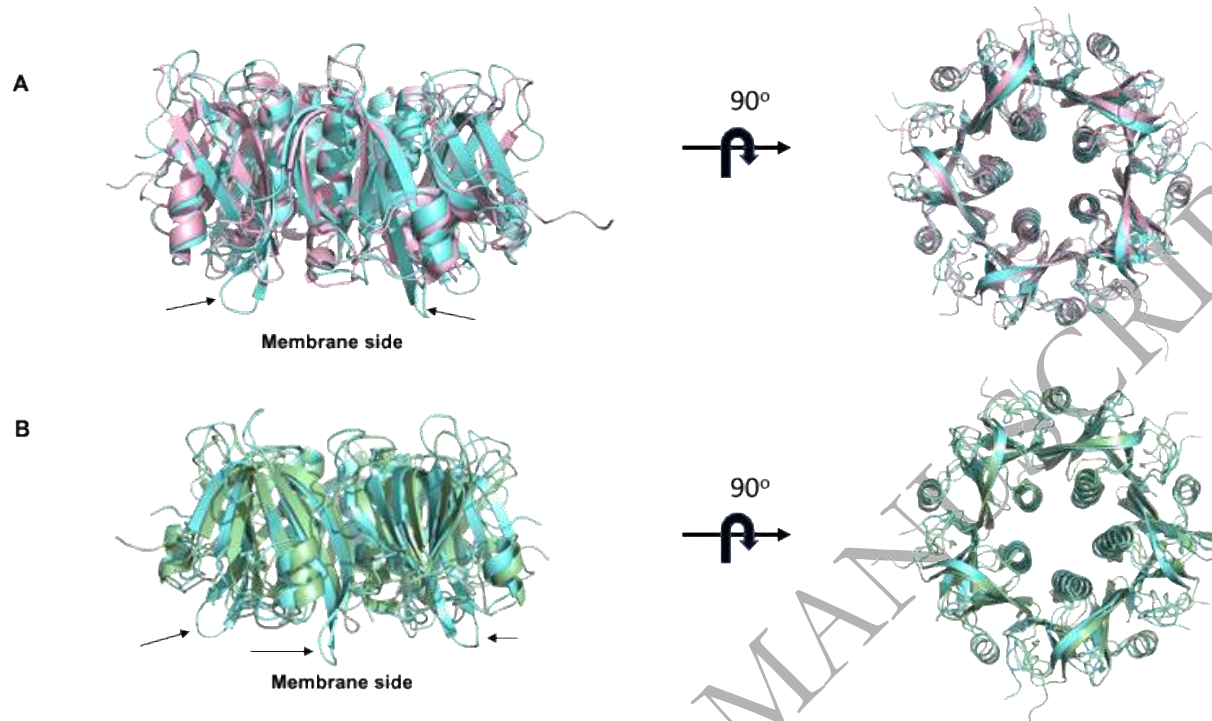


Fig. 8

1 SubB	EWTGDARDGMFSGVVITQFHTGQID---NKPYPFCEGKDSAGSS--ISACSNKNSSVWGASFSTLYNQALYFYTTGQPVRIYYEPGVWYTPPFVKALTSNALVGLSTOTTSTECFGPDRKKNSLE
2 Yerb	-----DTYYSNVIINWFSSGVYNSGGKDTTFFCIGYTRYGNKPDINWACKVDVYGKYNKGFSAWDTAKFYYSTGLQVRVYIKKDVWYDPAFRTGFSANELIAITSCSSHQYCVGPKLK-----

Fig. 9

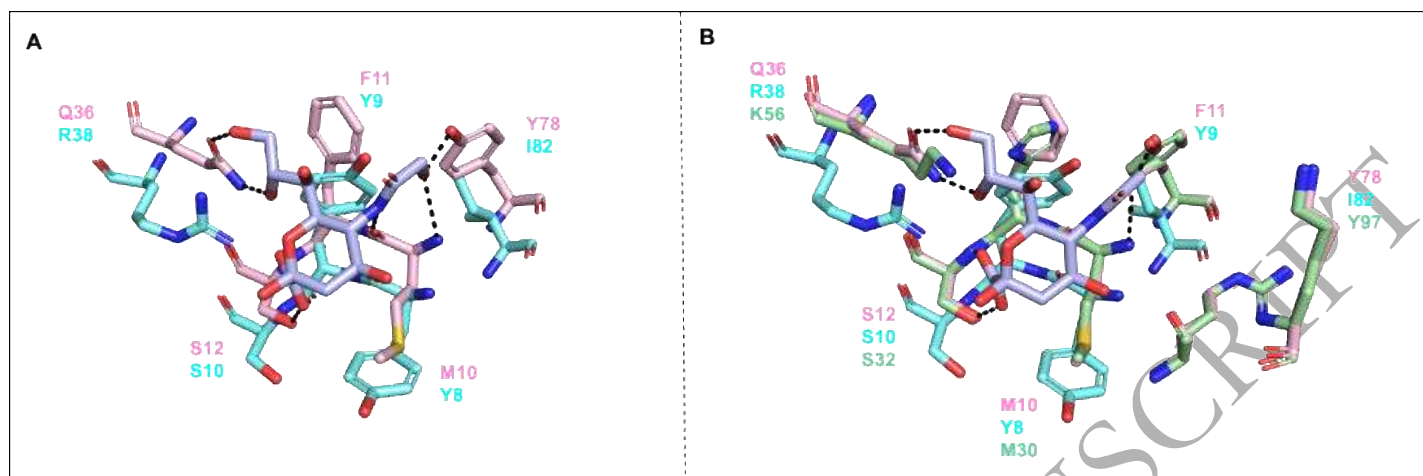
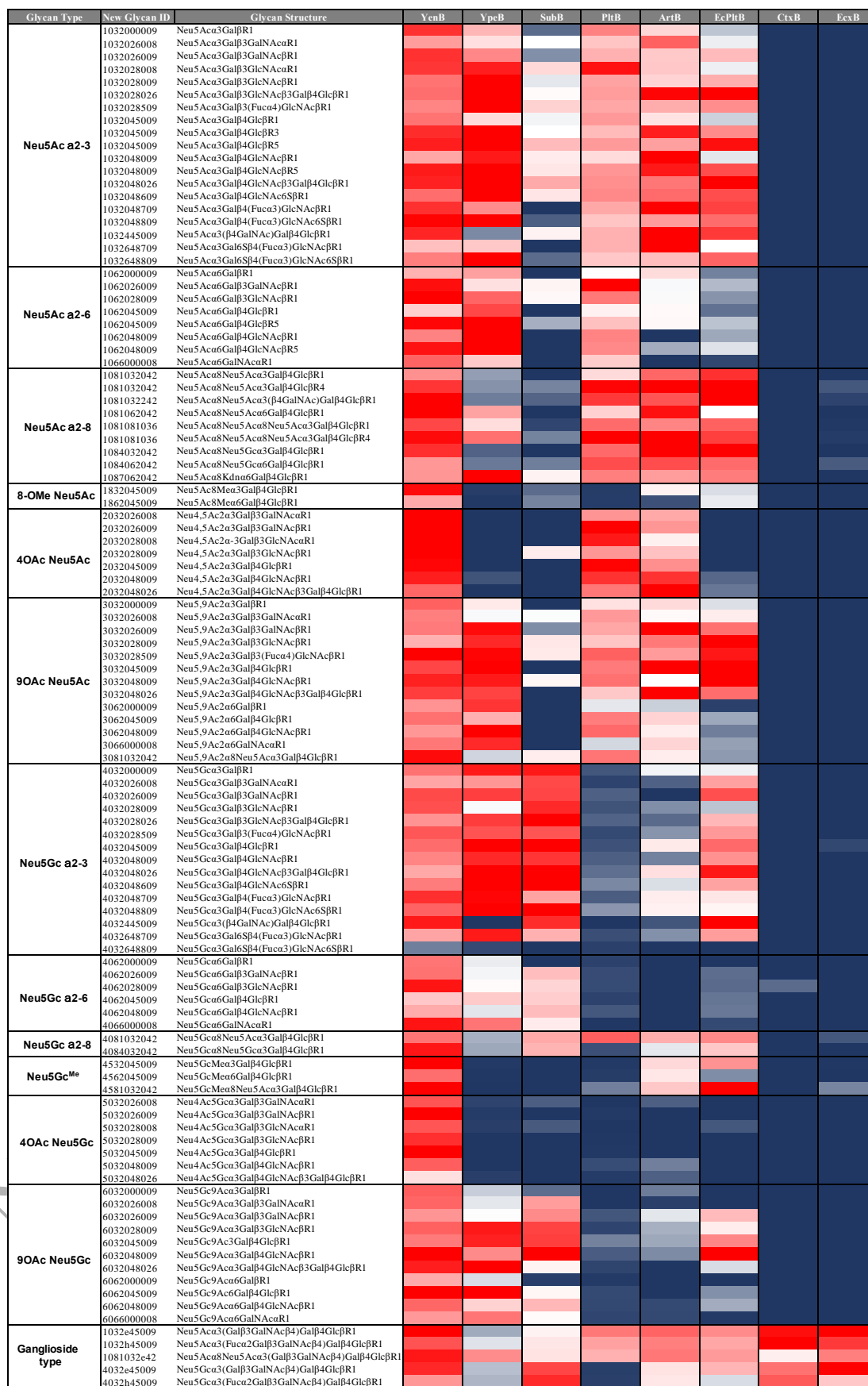


Fig. 10



Color scale
Min Max